Synthesis and Fluorescent Properties of Difluoroboron Dibenzoylmethane Polycaprolactone

Guoqing Zhang, Tyler L. St. Clair, and Cassandra L. Fraser*

Department of Chemistry, University of Virginia, Charlottesville, Virginia 22904

Received January 5, 2009; Revised Manuscript Received February 16, 2009

ABSTRACT: Difluoroboron β-diketonate dyes are noted for their intense fluorescence, one- and two-photon absorption, solvatochromism, and good aqueous stability. Incorporation of these dyes into polymers leads to processable optical materials, which in some cases display additional emissive features. For example, previously we reported that difluoroboron dibenzoylmethane−polylactide (BF_2dbmPLA) exhibits both fluorescence and room temperature phosphorescence (RTP). Typically RTP is ascribed to a matrix effect, where the rigid ordered medium restricts dye molecular motions, and excited-state decay via thermal pathways is hindered in favor of radiative decay. To test polymer effects on dye emissive properties, this study explores BF_2dbmPCL (PCL = poly(ε-caprolactone), a semicrystalline polymer) of different molecular weights ranging from ~3 to 18 kDa. PCL materials exhibit the expected intense fluorescence and molecular weight dependent emission but, surprisingly, no RTP. Phosphorescence is evident at lower temperatures (0 to −78 °C), however, and both intensities and lifetimes increase as the temperature is dropped. Polymer thermal properties were also examined. Aside from in the lowest molecular weight sample, the dye end group showed little effect on melting and glass transition temperatures. These dye-modified materials lend useful optical imaging capability to PCL, a polymer commonly used in drug delivery and tissue engineering applications.

Introduction

Many boron-containing materials possess impressive optical properties.[1,2] Luminescent difluoroboron complexes such as BODIPYs[3] and BF_2-β-diketonates (BF_2bdks)[4] exhibit large extinction coefficients and two-photon absorption cross section,[5] making them promising candidates for optical imaging and sensing applications. BODIPY derivatives are commercially available from Invitrogen as molecular probes that are functionalized to react with peptides and proteins for immunostaining due to their photophysical characteristics and water stability. Though BF_2bdks possess many useful optical properties, their potential has yet to be fully exploited for biological applications. In addition to high fluorescence quantum yields, which BF_2bdks share in common with BODIPYs, certain BF_2bdks, such as difluoroboron dibenzoylmethane (BF_2dbm) derivatives, also show pronounced room temperature phosphorescence (RTP) and delayed fluorescence (DF) when incorporated with polymer matrices in the solid state.[6] Furthermore, BF_2dbm fluorescence is dependent on fluorophore−fluorophore interactions[7] and molecular aggregation states,[8] revealing possibilities for emission tuning via engineering methods.

Previously we reported that the hydroxyl-functionalized BF_2dbm derivative, BF_2dbmOH, can be used to initiate tin-catalyzed, solvent-free, ring-opening polymerization of lactide. In the solid state, the resulting polymer, difluoroboron dibenzoylmethane polylactide (BF_2dbmPLA), exhibits polymer molecular weight tunable fluorescence and unusual, long-lived RTP under oxygen-free conditions.[7,8] As previously reported for other luminescent boron polymers,[1,2] covalent modification of BF_2dbm with PLA not only enhances the emitting properties of the boron dye but also lends processing advantages. The fluorescence quantum yield of BF_2dbm in CH_2Cl_2 is only 0.20,[4] but after modification, BF_2dbmPLA exhibits a roughly 4-fold increase (Φ_F ~0.85) under the same conditions due to the electron-donating alkoxy linker. By a simple strategy of nanoprecipitation,[9] BF_2dbmPLA can be conveniently fabricated as water-stable boron nanoparticles (BNPs) that retain all of the attractive bulk solid-state optical properties at the nanoscale and in aqueous environments.[10] Cellular uptake experiments indicate that BNPs are sufficiently small (~70 nm diameter) for intracellular imaging and sensing purposes. Given the emerging importance of nanoparticles in drug delivery,[11] tissue imaging,[12] and oxygen sensing,[13] biocompatible BNPs with tunable optical properties show promise for bionanotechnology.[14]

Our previous studies showed that the delayed emission from BF_2dbmPLA is absent in organic solvents such as CH_2Cl_2 even in degassed solutions.[6] In the solid state, in contrast, amorphous PLA made from DL-lactide serves as a rigid medium, which presumably reduces thermal vibrations and hinders quencher molecules from interacting with the dyes in the excited states, thus significantly boosting the radiative triplet yield. It has been reported that organized media[15] such as transparent crystals can also effectively enhance the phosphorescence yield via a similar matrix effect.[16] The drawback to employing multicomponent dye/matrix blends, however, is that processing can be more complex and homogeneity is hard to guarantee. Therefore, dye−crystalline polymer conjugates, with a combination of material organization and ease of fabrication, can be of great interest for generating RTP and harnessing it for practical applications. Such polymers possess highly organized regions from close packing of intra- and interchain segments, where the physical properties resemble those observed for crystals of small molecules.[17] One semicrystalline, biocompatible polymer commonly used in drug delivery systems and tissue engineering is poly(ε-caprolactone) (PCL).[18] PCL is commercially available in large scale, and its biodegradation has been studied in detail with regard to morphology and microbial variety.[19] In order to extend to a new material and to understand the effects of polymer composition and crystallinity on boron dye emission properties, in this study we explore the synthesis and optical properties of BF_2dbmPCL. Although both PCL and PLA are in the polyester genre and possess similar chemical properties, we show that the more crystalline PCL can alter the photophysical properties of BF_2dbm in dramatic ways.

* Corresponding author. E-mail: fraser@virginia.edu.

10.1021/ma900018r CCC: $40.75
Published on Web 03/26/2009

Experimental Section

Materials. The boron initiator BF_2dbmOH was prepared as previously reported.[6] ε-Caprolactone was dried over CaH_2 and distilled under reduced pressure prior to use. Tin(II) 2-ethylhexanoate ($Sn(oct)_2$, Spectrum) and all other reagents were used as received.

Methods. ^{1}H NMR (300 MHz) spectra were recorded on a Varian UnityInova spectrometer in $CDCl_3$ unless otherwise indicated. Resonances were referenced to the signal for residual protiochloroform at 7.260 ppm. ^{1}H NMR coupling constants are given in hertz. UV−vis spectra were recorded on a Hewlett-Packard 8452A diode-array spectrophotometer in CH_2Cl_2. Molecular weights were determined by three different methods: (1) GPC (THF, 25 °C, 1.0 mL/min) against polystyrene standards using an autosampler (BF_2dbmPCL molecular weights multiplied by 0.56 correction factor); (2) gel permeation chromatography (GPC) (THF, 25 °C, 1.0 mL/min) using multiangle laser light scattering (MALLS) (λ = 633 nm, 25 °C) and refractive index (RI) (λ = 633 nm, 40 °C) detection; (3) end group to polymer integration ratio from ^{1}H NMR spectra. A Polymer Laboratories 5 μm mixed-C guard column and two GPC columns along with Wyatt Technology Corp. (Optilab DSP interferometric refractometer, DAWN DSP laser photometer) and Agilent Technologies instrumentation (series 1100 HPLC) and Wyatt Technology software (ASTRA) were used in GPC analysis by Method 2. The incremental refractive indices (d*n*/d*c* values) for polymer samples were determined by a single injection method that assumed 100% mass recovery from the columns. Thermogravimetric analysis (TGA) was conducted using a TA Instruments TGA 2050 thermogravimetric analyzer from 30 to 500 °C with a heating/cooling rate of 10 °C/min under N_2. Differential scanning calorimetry (DSC) measurements were performed using a TA Instruments DSC 2920 modulated DSC. Analyses were carried out in modulated mode under a nitrogen atmosphere (amplitude = ±1 °C; period = 60 s; heating rate = 5 °C/min; range −10 to 200 °C). Reported values of thermal events are from the second heating cycle and the reversing heat flow curve unless indicated otherwise (T_d = onset point of decomposition; T_m reported as the peak maximum).

A Laurell Technologies WS-650S spin-coater was used to cast polymer films for luminescence measurements (4000 rpm). The photograph in Figure 6 was taken with a Canon Powershot SD600 Digital Elph camera on the automatic setting (no flash). Steady-state fluorescence emission spectra were recorded on a Horiba Fluorolog-3 Model FL3-22 spectrofluorometer (double-grating excitation and double-grating emission monochromators). Phosphorescence spectra were recorded with the same instrument except that a pulsed xenon lamp (λ_{ex} = 369 nm; duration <1 ms) was used, and spectra were collected with a 1 ms delay after excitation. Time-correlated single-photon counting (TCSPC) fluorescence lifetime measurements were performed with a NanoLED-370 (369 nm) excitation source and DataStation Hub as the SPC controller. Phosphorescence lifetimes were measured with a 500 ns multichannel scalar (MCS) excited with a pulsed xenon lamp (λ_{ex} = 369 nm; duration <1 ms). Lifetime data were analyzed with DataStation v2.4 software from Horiba Jobin Yvon. Variable temperature studies were conducted at 0 °C (ice bath), −42 °C (acetonitrile/dry ice), and −78 °C (acetone/dry ice).

BF_2dbmPCL (1). A representative procedure for the synthesis BF_2dbmPCL (**1**) (i.e., the low molecular weight sample) is provided. A dry Kontes flask was charged with BF_2dbmOH (0.056 g, 0.17 mmol) and ε-caprolactone (1.36 g, 11.9 mmol) under a nitrogen atmosphere. The flask was sealed and placed in an oil bath at 110 °C to create a homogeneous melt. Under a flow of nitrogen, a stock solution of $Sn(oct)_2$ (1.72 mg, 4.25 μmol) in hexanes was added to the reaction mixture. The reaction vessel was resealed and heated at 110 °C until an extremely viscous mixture resulted (~8 h). The reaction mixture was cooled to room temperature, dissolved in a minimal amount of CH_2Cl_2, and precipitated by dropwise addition to cold stirring hexanes (−78 °C). The supernatant was decanted, and the gummy residue was washed with cold hexanes and dried in vacuo to afford BF_2dbmPCL as a light yellow waxy solid: 0.32 g (22%; uncorrected for monomer consumption). ^{1}H NMR (300 MHz, $CDCl_3$): δ 8.16 (t, *J* = 9.0, 2′,6′-Ar*H*, 2″,6″-Ar*H*), 7.69 (t, *J* = 8.3, 4′-Ar*H*), 7.55 (m, 3″,5″-Ar*H*), 7.13 (s, COC*H*CO), 7.05 (d, *J* = 8.9, 3′,5′-Ar*H*), 4.48 (d, *J* = 4.5, CH_2CH_2OAr), 4.30 (m, CH_2CH_2OAr), 4.06 (t, *J* = 6.5, RCO_2CH_2), 2.31 (t, *J* = 7.5, CH_2CO_2R), 1.70−1.56 (m, CH_2), 1.43−1.32 (m, CH_2). Additional characterization data for BF_2dbmPCL samples (**1**−**5**) are summarized in Tables 1−3.

Table 1. Molecular Weight and UV/vis Spectral Data for BF_2dbmPCL (1−5)

	lactide[a] (equiv)	reaction time (h)	yield[b] (%)	M_n[c] (PS)	M_w[d] (MALLS)	M_n[e] (NMR)	PDI (PS/ MALLS)	ε[f] (M^{-1} cm^{-1})
1	70	8	22	1 600	3 000	1 400	1.11/1.04	35 900
2	130	17	42	5 400	6 500	6 900	1.17/1.05	34 500
3	150	24	68	9 000	10 400	12 300	1.24/1.07	34 500
4	275	48	53	11 800	14 200	15 600	1.35/1.10	28 200
5	400	72	48	16 400	18 200	24 900	1.31/1.10	31 400

[a] Per equivalent BF_2dbmOH initiator. [b] Uncorrected for monomer consumption. [c] GPC in THF vs polystyrene (PS) standards (0.56 correction factor applied). [d] GPC in THF. [e] In $CDCl_3$. [f] In CH_2Cl_2. λ = 396 nm.

Polymerization Kinetics. BF_2dbmOH (13.0 mg, 0.039 mmol), ε-caprolactone (0.67 g, 5.87 mmol), and $Sn(oct)_2$ (0.39 mg, 0.98 μmol) in hexanes were combined in a sealed Kontes flask under N_2. The entire bulb of the flask was submerged in a 110 °C oil bath. Aliquots were drawn up into a pipet tip at the specified times, and then the flask was resealed under nitrogen. Samples were analyzed by GPC (method 1, vs polystyrene standards) and by ^{1}H NMR spectroscopy (method 3, relative integration). Percent monomer consumption was obtained by comparing the integration of monomer vs (monomer + polymer) peaks via ^{1}H NMR spectroscopy. A first-order kinetics plot is provided in Figure 1, and an M_n vs % conversion in Figure 2.

Quantum Yield Measurements. Fluorescence quantum yields, Φ_F, for BF_2dbmPCL in CH_2Cl_2 were calculated versus anthracene in EtOH as a standard as previously described[20] using the following values: Φ_F(anthracene) = 0.27,[21] n_D^{20}(EtOH) = 1.360, n_D^{20}(CH_2Cl_2) = 1.424. Optically dilute CH_2CH_2 solutions of BF_2dbmPCL and EtOH solutions of the anthracene standard were prepared in 1 cm path length quartz cuvettes, and absorbances (A < 0.1) were recorded using a Hewlett-Packard 8452A UV/vis spectrometer. Steady-state emission spectra were obtained on a Horiba Fluorolog-3 Model FL3-22 spectrofluorometer (λ_{ex} = 350 nm; emission integration range: 365−700 nm).

Results and Discussion

The synthesis of BF_2dbmPCL was performed under solvent-free conditions using BF_2dbmOH as the initiator and $Sn(oct)_2$ as the catalyst (eq 1). Figure 1 shows the kinetics plot of the polymerization of ε-caprolactone using a catalyst loading of 1:40 $Sn(oct)_2$:BF_2dbmOH. The rate of polymerization is perceivably slower than that of lactide.[6] The plot starts to deviate from linearity beyond ~11 h, indicating decreased molecular weight control. Figure 2 shows a molecular weight vs percent conversion plot for this reaction determined via GPC (THF vs PS standard). The data can be compared to the expected result for a controlled system, calculated based on monomer to initiator loading, and indicated by the diagonal line. Although the data for this sample reveal a consistently lower molecular weight than expected at any given conversion percentage, perhaps due to discrepancies between PCL and PS standards, the relationship is roughly linear until about 85% conversion, with PDIs maintained below 1.2. (Note that NMR and GPC molecular weights for preparative scale reactions (Table 1) show greater correspondence with calculated M_n values.)

Preparative scale reactions were also performed to generate BF_2dbmPCL polymers (**1**−**5**) of various molecular weights. Polymers were characterized by GPC and NMR spectroscopy. An overlay of GPC traces for **1**−**5** is shown in Figure 3. For low molecular weight samples, the peaks are fairly symmetric;

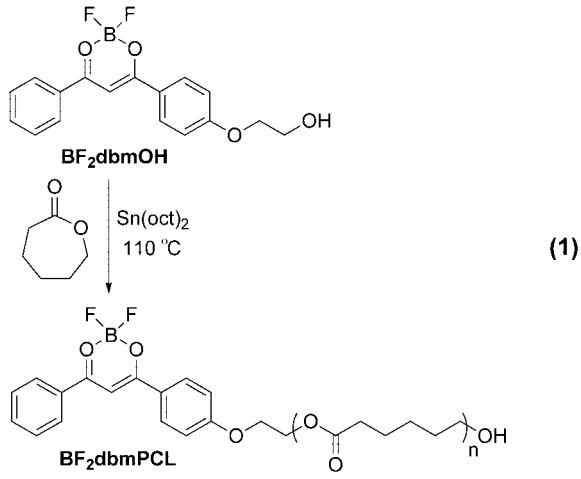

(1)

however, high molecular weight shoulders are present in samples of higher molecular weights. This is likely due to side reactions, such as transesterification, for extended polymerization times in a highly viscous system. A representative ^{1}H NMR spectrum of BF_2dbmPCL is shown in Figure 4. The end group is clearly evident so that molecular weight can be determined by relative integration of resonances at 8.16 and 2.31 ppm corresponding to dbm aromatic and PCL $-CH_2CO_2R$ protons, respectively (Table 1). Further, the covalent attachment is substantiated by the spectral shift of the methylene groups, e.g., from 4.04 ppm ($ArOCH_2CH_2OH$) in the boron initiator to 4.48 ppm ($ArOCH_2CH_2OPCL$) in the dye−polymer conjugate.

Thermal properties of purified polymers were also examined (Table 2). Because PCL is a semicrystalline polymer, distinct T_m peaks were observed for all five samples. Except for the very low molecular weight sample **1**, which has significantly decreased melting and decomposition temperatures (T_m = 39/44 and T_d = 305), the other BF_2dbmPCL samples have similar T_m and T_d values of ∼55 and ∼355 °C, respectively. These values are in accord with previously reports for PCL.[22] The glass transition temperature T_g of PCL is reported to be below −60 °C;[18] therefore, we were unable to determine the T_g with the current instrument setup (lower limit: −20 °C). These findings indicate that boron dye end-functionalization has little effect on the thermal behavior of PCL polymers except at high dye/polymer loading.

The optical properties of BF_2dbmPCL polymers were investigated in CH_2Cl_2. As expected, the UV/vis absorbance is comparable to the BF_2dbmOH initiator with a strong $\pi-\pi^*$ transition at 396 nm. This suggests that the PCL tail barely affects the electronic transitions of the dye. The molar extinction coefficients at 396 nm for the five boron polymers range from 28 200 to 35 900 M^{-1} cm^{-1} (Table 1), values comparable with those found for BF_2dbmPLA in CH_2Cl_2. Although values drop slightly for higher molecular weight samples **4** and **5**, even still, these results confirm the integrity of the dye in a majority of the sample even after days at 110 °C. The solution absorption and emission spectra for all five BF_2dbmPCL polymers are nearly identical with emission maxima, λ_{em}, at ∼430 nm (Table 3). A representative example is given in Figure 5. No delayed emission was observed for any of the samples, not even in degassed solution. Fluorescence lifetimes for BF_2dbmPCL solutions are comparable to the dye initiator (τ = 2.0 ns)[6] and to a previously reported BF_2dbmPLA molecular weight series (τ = 1.9−2.0 ns).[7] Quantum yields (Φ_F) for BF_2dbmPCL (54−72%) are slightly lower than for BF_2dbmPLA under similar conditions (77−89%).[6,7]

The emissive properties of BF_2dbmPCL were also examined in the solid state via luminescence spectroscopy and lifetime measurements (Table 3). Like BF_2dbmPLA,[7] BF_2dbmPCL exhibits varying emission colors depending on the molecular weight (Figure 6). That lower molecular weight BF_2dbmPCL has red-shifted emission suggests similar fluorophore−fluorophore (F−F) interactions and excited-state stabilization in the PCL system. The fluorescence emission spectra for BF_2dbmPCL powders are shown in Figure 7A. The emission maxima range from 523 nm (M_n = 1600 Da) to 438 nm (M_n = 16 400 Da). Unlike BF_2dbmPLA, which showed progressively shifting emission maxima,[7] BF_2dbmPCL powders resemble a bimodal monomer−excimer system where two emission bands at fixed wavelength change in relative intensities. This difference of fluorescence spectra between BF_2dbmPLA and BF_2dbmPCL is likely to be caused by the morphological difference between PLA and PCL. Because the DL−PLA is amorphous, the dye may be evenly dispersed throughout the solid substrate. For PCL, dye molecules may distribute unevenly in amorphous and crystalline regions. The excitation spectra for **1** and **5** are shown

Table 2. Thermal Analysis Data for BF_2dbmPCL Samples (1−5)

	T_d (°C)	T_m (°C)
1	305	39/44
2	342	53
3	355	55
4	361	55
5	356	56

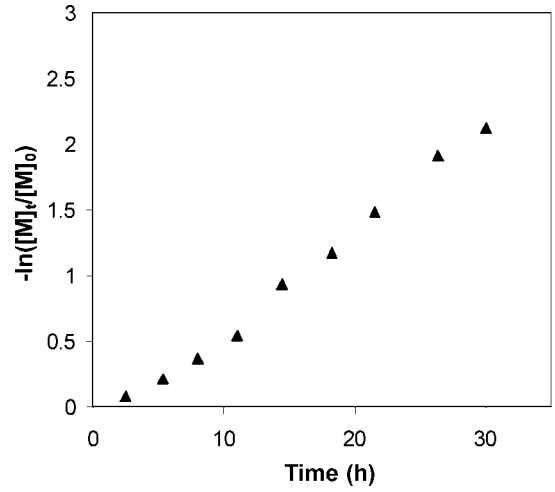

Figure 1. Kinetics plot for the solvent-free polymerization of ε-caprolactone (1:40:150 $Sn(oct)_2$:BF_2dbmOH:lactide).

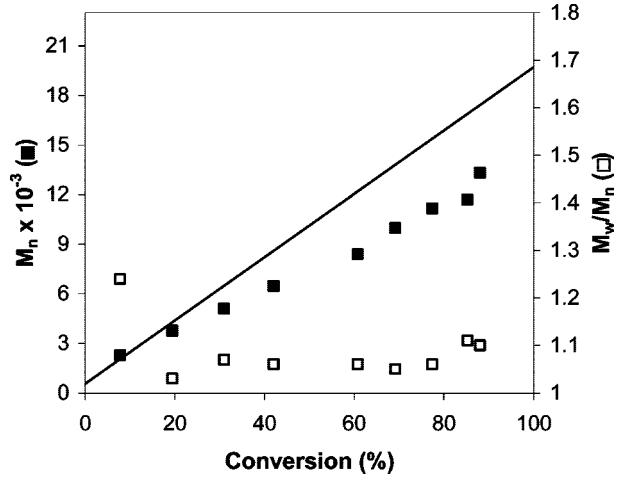

Figure 2. BF_2dbmPCL number-average molecular weights (■) and polydispersity indices (M_w/M_n, □) vs percent monomer conversion (1:40:150 $Sn(oct)_2$:BF_2dbmOH:lactide; via GPC vs PS standards). Solid line represents the calculated M_n value.

Table 3. Fluorescence Data for BF_2dbmPCL Solutions, Powders, and Films

	solutions			powders				films			
	λ_{em}[a] (nm)	τ[b] (ns)	ϕ_F[c]	λ_{em}[a] (nm)	τ[d] (ns)	%[e]	τ_{pw0}[f] (ns)	λ_{em}[a] (nm)	τ[d] (ns)	%[e]	τ_{pw0}[f] (ns)
1	429	1.91	0.61	526	0.23	4	32.0	523	2.59	8	31.2
					7.93	17			14.1	27	
					38.8	79			41.8	65	
2	430	1.92	0.55	497	0.83	4	25.2	457	0.63	41	6.06
					7.56	27			4.19	34	
					33.5	69			17.5	25	
3	430	1.91	0.72	459	0.90	14	15.6	442	0.64	57	2.31
					6.27	36			2.32	28	
					26.4	50			8.64	15	
4	430	1.92	0.62	449	1.12	46	6.10	439	1.04	65	1.82
					4.78	34			2.15	21	
					19.8	20			4.99	14	
5	429	1.93	0.54	447	0.12	7	2.13	438	0.05	20	1.35
					1.52	72			1.52	76	
					4.93	21			4.68	4	

[a] In CH_2Cl_2, excited at 369 nm LED. [b] Excitation source: 369 nm LED, single-exponential decay. [c] Fluorescence quantum yields relative to anthracene in EtOH.[21] [d] Excitation source: 369 nm LED, triple-exponential decay. [e] Percentages represent pre-exponential weighted values. [f] Pre-exponential weighted lifetimes.[23]

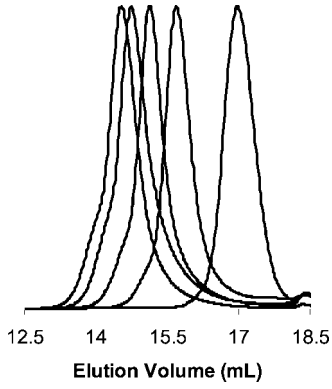

Figure 3. GPC (RI) overlay of BF_2dbmPCL polymers **1**−**5** (right to left) in THF.

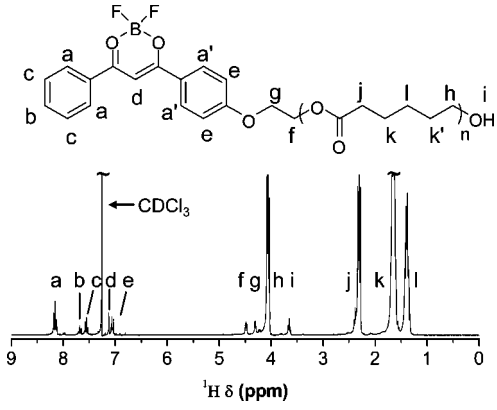

Figure 4. Representative ^{1}H NMR spectrum of BF_2dbmPCL (**1**) in $CDCl_3$ (peak labels a and k also designate overlapping a′ and k′ peaks).

in Figure 8. Compared to **5**, the spectrum for **1** not only varies in vibrational structure but also is significantly broadened in the lower energy region (430−450 nm). This may suggest the existence of ground-state interactions in addition to possible excited-state coupling among boron fluorophores in the PCL matrix.

The lifetimes of the powder emission were also measured with excitation at 369 nm (Table 3). Lower molecular weight samples exhibit much longer-lived fluorescence lifetimes; the pre-exponential weighted lifetime[23] for **1** (32.0 ns) is more than 15 times that for **5** (2.13 ns). This observation is consistent with BF_2dbmPLA powders, which also show molecular weight

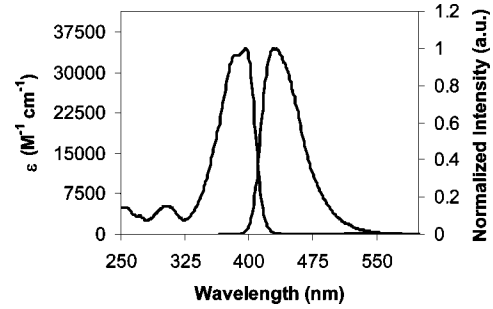

Figure 5. Absorption (left) and emission spectra (right) for BF_2dbmPCL (**2**) in CH_2Cl_2 solution.

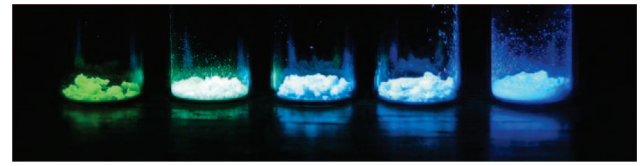

Figure 6. Image showing emission color tuning for BF_2dbmPCL in the solid state as powders (**1**−**5** left to right).

dependent fluorescence lifetimes. All lifetime decays can be fit with triple exponentials, which is common for heterogeneous solid polymer substrates.[24] In our previous report, we have ascribed the longer lived components to fluorophore−fluorophore (F−F) interactions.

The fluorescent spectra for the spin-cast films of BF_2dbmPCL (**1**−**5**) were also investigated (Figure 7B, Table 3). The low optical density (abs < 0.1) of the films may minimize spectral and lifetime distortions caused by self-absorption.[25] Like the powders, the films show a decreasing trend in both λ_{max} (523 to 438 nm) and τ_{pw0} (31.2 to 1.35 ns) from **1** to **5**. There are some differences in the shapes of the spectra, however, especially for **3**, which for the powder has a much more significant low-energy shoulder. These findings are consistent with the previous results obtained for BF_2dbmPLA solid-state emission.[7] It is quite common that processing conditions and mechanical stimuli can alter the emissive properties of heterogeneous polymeric materials.[26] Excimeric interactions, relative fluorophore orientations, or material/substrate interactions could all contribute to the observed optical differences.

Under inert atmospheres (i.e., low or no O_2), we had anticipated strong RTP for BF_2dbmPCL in the solid state, given that PCL has organized crystalline regions, corresponding to a

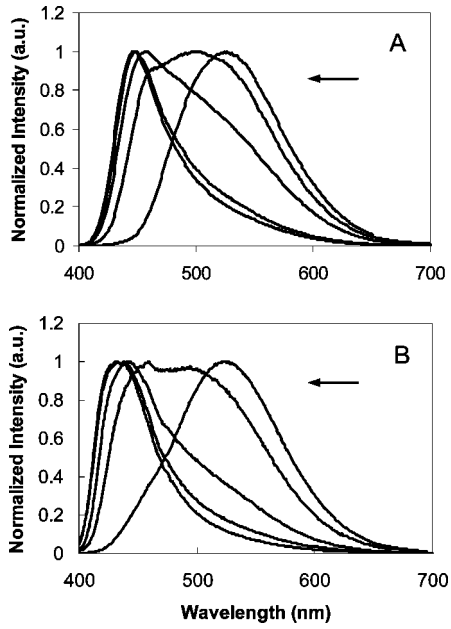

Figure 7. Fluorescence emission spectra of BF_2dbmPCL powders (A) and films (B) (**1**−**5** indicated by the arrow, right to left).

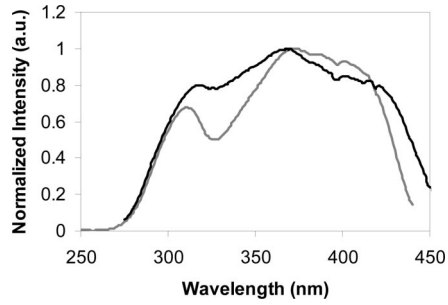

Figure 8. Excitation spectra of BF_2dbmPCL powders **1** (black) and **5** (gray).

more rigid dye environment. Again, embedding dyes in ordered media such as cyclodextrins,[27] glucose glass,[28] proteins,[29] or micelles[30] can increase the likelihood of room temperature phosphorescence. But surprisingly, no delayed emission was observed for the BF_2dbmPCL samples! One possible explanation for this observation is that the striking difference between PLA and PCL with respect to triplet emission may stem from differences in the polymer morphological states at room temperature. It is well-known that below the glass transition temperature, T_g, amorphous polymers or the amorphous regions of semicrystalline polymers are in a rigid "glassy" state characterized by a small polymer free volume V_f. In this state, polymer main chains are "frozen" and interchain motions are diminished.[31] Assuming the dye molecules are distributed in this region, the BF_2dbm chromophore in the excited stated, more restricted from vibrations and other molecular motions, may decay mainly via the radiative pathway, i.e., RTP for triplet radiative decay. Above T_g, these "frozen" regions become rubbery and polymer chains have much more freedom of motion including interchain gliding. The average interstitial space, V_f, is also increased due to more significant polymer chain movements. Therefore, thermal decay may become competitive with or dominate triplet excited-state radiative decay above this temperature, given the very slow RTP decay (τ_P ~200 ms for PLA samples).

According to this hypothesis, radiative triplet decay is unlikely above the glass transition temperature. As mentioned above, PCL has a T_g value below −60 °C, well below room temperature, whereas the T_g of PLA is ~60 °C. In fact, for BF_2dbmPLA, the phosphorescence "afterglow" disappears above 60 °C. The absence of RTP for BF_2dbmPCL suggests that the dye might not reside primarily in the crystalline regions, but instead in the interstitial spaces between ordered microdomains. This is also consistent with the fluorescence spectra for BF_2dbmPCL, too. At similar molecular weights, BF_2dbmPCL has a more broadened and red-shifted emission than its BF_2dbmPLA counterpart. If the dyes are excluded from certain regions (crystalline), their concentrations increase in the other regions (amorphous), leading to increased F−F interactions and, consequently, stabilization of the singlet excited-state and red-shifted emission. This may also explain the broadened excitation spectra for the lower MW samples, where close fluorophore contacts in the amorphous region lead to ground-state interactions or excited-state excimer formation.

Table 4. Phosphorescence Lifetime Decay Data for BF_2dbmPCL (3) at Different Temperatures

temp[a] (°C)	λ_{max}[b] (nm)	τ_P[c] (ms)[b]	(%)	χ^2	τ_{pw0}[d] (ms)
0	531	6.4	10	1.23	123.6
		56.9	45		
		219.9	45		
−42	519	16.0	2	1.19	671.8
		236.3	22		
		816.2	76		
−78	518	32.0	1	1.05	1327.3
		425.6	10		
		1441.4	89		

[a] Measurements were taken after 5 min to allow for temperature stabilization. [b] Excited at 369 nm. [c] Percentages represent pre-exponential weighted values. [d] Pre-exponential weighted lifetimes.[23]

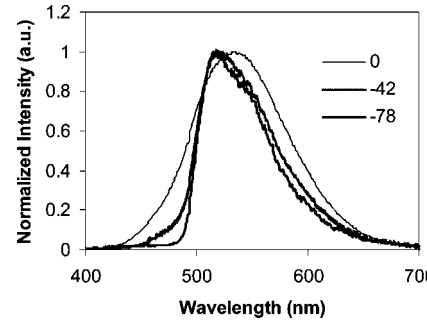

Figure 9. Phosphorescence spectra at 0, −42, and −78 °C for BF_2dbmPCL (**3**) (delay time after excitation: 10 ms).

To examine the temperature effects for BF_2dbmPCL, the emission spectra (Figure 9) and lifetime data were measured for polymer **3** (M_n = 9000 Da) at three temperatures (0, −42, and −78 °C) (Table 4). Although both film and powder samples both display phosphorescence at lower temperatures, this variable temperature study was performed for the powder because of the much stronger signal intensity compared to films. Measurements were run under nitrogen to prevent oxygen quenching of the triplet state. The spectra were collected with a 10 ms delay to capture phosphorescence independently of short-lived fluorescence. As the temperature was decreased, both the phosphorescence intensity and lifetime increased significantly (Table 4). Although we had expected the appearance of phosphorescence below PCL T_g = −60 °C, these observations show that the onset of phosphorescence appears at even higher temperatures, perhaps when the PCL solid-state solvent is viscous enough. Weak phosphorescence was already visually evident in an ice−water bath (0 °C). As the temperature was lowered, the shape of the corresponding spectrum became narrower, accompanied by the emission maximum shifted to the blue (λ_{max} 0 °C: 531 nm; −42 °C: 520 nm; and −78 °C: 518 nm). The broadening of the spectra at higher temperatures

could be due, in part, to the overlap from thermally repopulated temperature-dependent delayed fluorescence.[7] Alternatively, at lower temperature, the rigidochromic effect[32] may be responsible for the hypsochromic shift. One noticeable difference between BF_2dbmPLA and BF_2dbmPCL is that although PCL and PLA have similar chemical composition and polarity, the phosphorescence emission of BF_2dbmPCL (519 nm) is perceivably red-shifted compared to BF_2dbmPLA (509 nm) at 0 °C. This could indicate either triplet relaxation is more prominent in the PCL matrix or that the triplet energy is lower from enhanced F−F interactions.

Emission lifetimes are also very sensitive to the temperature,[33] which has been observed for a wide variety of luminophores, both for organic and metal[34] compounds. At 0 °C, the decay dynamics are complex and can be fitted with a triple-exponential decay with $\chi^2 = 1.23$. The preexponential-weighted lifetime τ_{pw0} was found to be 123.6 ms. When the temperature is lowered from 0 to −78 °C, the lifetime increases by more than 10-fold. Clearly, polymer matrix effects on boron dye optical properties are complex and merit further investigation.

Conclusion

Boron dye polymer conjugates, BF_2dbmPCL, were generated by the solvent-free $Sn(oct)_2$-catalyzed polymerization of ε-caprolactone using BF_2dbmOH, a hydroxy-functionalized boron initiator. Like previously reported polylactide analogues,[6,7] BF_2dbmPCL exhibits intense blue fluorescence upon UV excitation and materials show blue-shifted emission with increasing molecular weight. Polymer thermal properties and dye optical properties show the most dramatic differences for the low molecular weight sample (i.e., high dye loading). However, unlike BF_2dbmPLA which displays unusual phosphorescence at room and even body temperature (i.e., 37 °C), for the PCL derivative, phosphorescence is only evident at depressed temperatures (i.e., at 0, −42, and −78 °C, examined in this study.) This was surprising, given that the chemical composition of these biodegradable polyesters are quite similar and that RTP is generally enhanced in rigid, organized media, and semicrystalline PCL is more ordered than amorphous DL-PLA. However, the T_g for PLA is above room temperature, whereas that for PCL is significantly below room temperature, and this transition along with increased viscosity at lower temperature may also be playing a role. Additional studies are merited with different boron diketonate dye analogues and solid-state matrices to better understand the effects of polymer composition and physical properties on boron dye emission. Processing of dye−polymer conjugates for imaging, drug delivery, and tissue engineering applications is underway.

Acknowledgment. We thank the National Science Foundation (CHE 0718879) for support for this work.

References and Notes

(1) (a) Nagata, Y.; Otaka, H.; Chujo, Y. *Macromolecules* **2008**, *41*, 737–740. (b) Nagai, A.; Kodado, K.; Nagata, Y.; Chujo, Y. *Macromolecules* **2008**, *41*, 8295–8298.
(2) (a) Qin, Y.; Kiburu, I.; Shah, S.; Jäkle, F. *Macromolecules* **2006**, *39*, 9041–9048. (b) Parab, K.; Venkatasubbaiah, K.; Jäkle, F. *J. Am. Chem. Soc.* **2006**, *128*, 12879–12885. (c) Jäkle, F. *Coord. Chem. Rev.* **2006**, *250*, 1107–1121.
(3) Loudet, A.; Burgess, K. *Chem. Rev.* **2007**, *107*, 4891–4932.
(4) Cogné-Laage, E.; Allemand, J.-F.; Ruel, O.; Baudin, J.-B.; Croquette, V.; Blanchard-Desce, M.; Jullien, L. *Chem.— Eur. J.* **2004**, *10*, 1445–1455.
(5) Risko, C.; Zojer, E.; Brocorens, P.; Marder, S. R.; Brédas, J. L. *Chem. Phys.* **2005**, *313*, 151–157.
(6) Zhang, G.; Chen, J.; Payne, S. J.; Kooi, S. E.; Demas, J. N.; Fraser, C. L. *J. Am. Chem. Soc.* **2007**, *129*, 8942–8943.
(7) Zhang, G.; Kooi, S. E.; Demas, J. N.; Fraser, C. L. *Adv. Mater.* **2008**, *20*, 2099–2104.
(8) Mirochnik, A.; Fedorenko, E.; Kuryavyi, V.; Bukvetskii, B.; Karasev, V. *J. Fluoresc.* **2006**, *16*, 279–286.
(9) Bilati, U.; Allémann, E.; Doelker, E. *Eur. J. Pharm. Sci.* **2005**, *24*, 67–75.
(10) Pfister, A.; Zhang, G.; Zareno, J.; Horwitz, A. F.; Fraser, C. L. *ACS Nano* **2008**, *2*, 1252–1258.
(11) Sahoo, S. K.; Labhasetwar, V. *Drug Discovery Today* **2003**, *8*, 1112–1120.
(12) Gao, X.; Yang, L.; Petros, J. A.; Marshall, F. F.; Simons, J. W.; Nie, S. *Curr. Opin. Biotechnol.* **2005**, *16*, 63–72.
(13) Xu, H.; Aylott, J. W.; Kopelman, R.; Miller, T. J.; Philbert, M. A. *Anal. Chem.* **2001**, *73*, 4124–4133.
(14) Roco, M. C. *Curr. Opin. Biotechnol.* **2003**, *14*, 337–346.
(15) Arancibia, J. A.; Escandar, G. M. *Analyst* **2001**, *126*, 917–922.
(16) Mitchell, C. A.; Gurney, R. W.; Jang, S.-H.; Kahr, B. *J. Am. Chem. Soc.* **1998**, *120*, 9726–9727.
(17) Bower, D. I. *An Introduction to Polymer Physics*; Cambridge University Press: New York, 2002; pp 87−160.
(18) Pitt, C. G. In *Drugs and Pharmaceutical Sciences*; Chasin, M., Langer, R., Eds.; Marcel Dekker: New York, 1990; Vol. 45, pp 71−120.
(19) (a) Benedict, C. V.; Cook, W. J.; Jarrett, P.; Cameron, J. A.; Huang, S. J.; Bell, J. P. *J. Appl. Polym. Sci.* **1983**, *28*, 327–334. (b) Benedict, C. V.; Cameron, J. A.; Huang, S. J. *J. Appl. Polym. Sci.* **1983**, *28*, 335–342.
(20) Demas, J. N.; Crosby, G. A. *J. Phys. Chem.* **1971**, *75*, 991–1024 (section II.C.2, eq 16.).
(21) Dawson, W. R.; Windsor, M. W. *J. Phys. Chem.* **1968**, *72*, 3251–3260.
(22) Huang, M.-H.; Li, S.; Coudane, J.; Vert, M. *Macromol. Chem. Phys.* **2003**, *204*, 1994–2001.
(23) Carraway, E. R.; Demas, J. N.; DeGraff, B. A.; Bacon, J. R. *Anal. Chem.* **1991**, *63*, 337–342.
(24) Xu, W.; Schmidt, R.; Whaley, M.; Demas, J. N.; DeGraff, B. A.; Karikari, E. K.; Farmer, B. L. *Anal. Chem.* **1995**, *67*, 3172–3180.
(25) Hehlen, M. P. *J. Opt. Soc. Am. B* **1997**, *14*, 1312–1318. (b) Kobayashi, T.; Nagakura, S. *Mol. Cryst. Liq. Cryst.* **1974**, *26*, 33–43.
(26) (a) Schwartz, B. J. *Annu. Rev. Phys. Chem.* **2003**, *54*, 141–172. (b) Shi, Y.; Liu, J.; Yang, Y. *J. Appl. Phys.* **2000**, *87*, 4254–4263. (c) Wang, Y.; Park, J. S.; Leech, J. P.; Miao, S.; Bunz, U. H. F. *Macromolecules* **2007**, *40*, 1843–1850.
(27) Li, S.; Purdy, W. C. *Chem. Rev.* **1992**, *92*, 1457–1470.
(28) Wang, J.; Hurtubise, R. J. *Anal. Chem.* **1997**, *69*, 1946–1951.
(29) Saviotti, M. L.; Galley, W. C. *Proc. Natl. Acad. Sci. U.S.A.* **1974**, *71*, 4154–4158.
(30) Love, L. J. C.; Skrilec, M.; Habarta, J. G. *Anal. Chem.* **1980**, *52*, 754–759.
(31) Gibbs, J. H.; DiMarzio, E. A. *J. Chem. Phys.* **1958**, *28*, 373–383.
(32) Peinado, C.; Salvador, E. F.; Catalina, F.; Lozano, A. E. *Polymer* **2001**, *42*, 2815–2825.
(33) Lakowicz, J. R. *Principles of Fluorescence Spectroscopy*; 3rd ed.; Springer: New York, 2006; pp 63−154, 205−275.
(34) Evans, R. C.; Douglas, P.; Winscom, C. J. *Coord. Chem. Rev.* **2006**, *250*, 2093–2126.

MA900018R